



HAL
open science

Characterization of the mass transfer fluxes in a capacitive desalination cell by using FeIII(CN)6³⁻/FeII(CN)6⁴⁻ redox couple as an electrochemical probe

Assane Sene, Barbara Daffos, Pierre-Louis Taberna, Patrice Simon

► **To cite this version:**

Assane Sene, Barbara Daffos, Pierre-Louis Taberna, Patrice Simon. Characterization of the mass transfer fluxes in a capacitive desalination cell by using FeIII(CN)6³⁻/FeII(CN)6⁴⁻ redox couple as an electrochemical probe. *Journal of Electroanalytical Chemistry*, 2019, 842, pp.127-132. 10.1016/j.jelechem.2019.04.060 . hal-02308337

HAL Id: hal-02308337

<https://hal.science/hal-02308337>

Submitted on 8 Oct 2019

HAL is a multi-disciplinary open access archive for the deposit and dissemination of scientific research documents, whether they are published or not. The documents may come from teaching and research institutions in France or abroad, or from public or private research centers.

L'archive ouverte pluridisciplinaire **HAL**, est destinée au dépôt et à la diffusion de documents scientifiques de niveau recherche, publiés ou non, émanant des établissements d'enseignement et de recherche français ou étrangers, des laboratoires publics ou privés.



Open Archive Toulouse Archive Ouverte (OATAO)

OATAO is an open access repository that collects the work of Toulouse researchers and makes it freely available over the web where possible

This is an author's version published in: <http://oatao.univ-toulouse.fr/24344>

Official URL: <https://doi.org/10.1016/j.jelechem.2019.04.060>

To cite this version:

Sene, Assane  and Daffos, Barbara  and Taberna, Pierre-Louis  and Simon, Patrice  *Characterization of the mass transfer fluxes in a capacitive desalination cell by using FeIII(CN)6³⁻/FeII(CN)6⁴⁻ redox couple as an electrochemical probe.* (2019) *Journal of Electroanalytical Chemistry*, 842. 127-132. ISSN 1572-6657

Any correspondence concerning this service should be sent to the repository administrator: tech-oatao@listes-diff.inp-toulouse.fr

Characterization of the mass transfer fluxes in a capacitive desalination cell by using $\text{Fe}^{\text{III}}(\text{CN})_6^{3-}/\text{Fe}^{\text{II}}(\text{CN})_6^{4-}$ redox couple as an electrochemical probe

Assane Sene, Barbara Daffos, Pierre-Louis Taberna, Patrice Simon*

CIRIMAT, Université de Toulouse, CNRS, INPT, UPS, 118 route de Narbonne, 31062 Toulouse Cedex 9, France
Réseau sur le Stockage Electrochimique de l'Energie (RS2E), FR CNRS 3459, 80039 Amiens Cedex, France

ARTICLE INFO

Keywords:

Cyclic voltammetry
Mass transfer
Desalination
Flow
Activated carbon

ABSTRACT

This paper focuses on the characterization of an electrochemical flow cell designed for capacitive desalination, by using the $\text{Fe}^{\text{III}}(\text{CN})_6^{3-}/\text{Fe}^{\text{II}}(\text{CN})_6^{4-}$ redox couple as an electrochemical probe. A relationship between the potential scan rate and the electrolyte flow rate has been first established by defining a dimensionless number, θ . Depending on the θ values, two regime domains – dependent and non-dependent from the flow rate - have been defined. The dimensionless number θ was found to be of great help for defining the suitable flow rate for several carbon based electrodes exhibiting different surface area, using $\text{Fe}^{\text{III}}(\text{CN})_6^{3-}/\text{Fe}^{\text{II}}(\text{CN})_6^{4-}$ redox couple as an electrochemical probe. The proposed electrochemical analysis is a way to optimize the performance of an electrochemical flow cell for capacitive desalination applications.

1. Introduction

97% of the global water resources on earth is salted, 2% is locked in the glaciers and ice caps and only about 1% is present as fresh liquid water [1]. As a result, millions of people around the world do not have access to safe drinking water. Several techniques for water desalination have been developed to solve this problem [2–4]. As one of these techniques, capacitive desalination, which aims at adsorbing Na^+ and Cl^- ions onto high surface area porous carbons under polarization, has proved to be efficient for desalination of seawater [5–7]. In capacitive desalination process, Na^+ ions migrate and are adsorbed (trapped) into the porosity of the negative electrode as a result of an applied potential from an external source (power generator), while Cl^- do the same at the positive electrode. The optimization of the desalination performance needs fine-tuning of key parameters such as, among others, the selection of the porous carbon and the cell design [8–12]. The nature of the electrode used has a substantial impact on the electrochemical reaction efficiency. Using flat platinum foils as working electrode, electrochemical processes – capacitive storage and redox reactions – take place at the surface of the electrode. When using porous electrode, the surface is massively increased – some activated carbons used exhibit $> 1000 \text{ m}^2/\text{g}$ – but the mass transport parameters within the porous network of the electrode affects the electrochemical performance [13–15].

This study aims at assessing the desalination cell efficiency, that is

to say, to optimize the charge exchanged. A relationship between the potential scan rate and the electrolyte flow rate has been first defined through an adimensional number θ , which allow to identify two different regimes in the cell, i.e., a permanent – flow rate dependent – and a non-permanent regime – flow rate independent. The different operating domains of the desalination cell have been analyzed at the light of the θ value, using $\text{Fe}^{\text{III}}(\text{CN})_6^{3-}/\text{Fe}^{\text{II}}(\text{CN})_6^{4-}$ redox couple as an electrochemical probe. This study has been made using three different working electrodes: a flat Pt foil – for sake of comparison – a platinum foil covered first with carbon black and then with a high surface area porous carbon. The objective will be to assess the influence of the surface area on the electrochemical performance of the electrode under various regimes (electrolyte low and potential scan rates).

2. Experimental

The electrochemical cell used, shown in Fig. 1a, contains two compartments - an anolyte and a catholyte of 560 μL each - consisting in a Plexiglas™ body. As depicted in Fig. 1b, each compartment exhibits a width (W) of 4 mm and a length (L) of 35 mm. A 100 μm -thick platinum (Pt) current collector (Fig. 1a, (2)) is placed in these cavities; 1 mm-thick silicone seal (Fig. 1a, (3)) with a hole conformal to the cavity is deposited on the Plexiglas body. As a result, each compartment has a total depth (h) of 3 mm. The two compartments are separated by two layers of porous PVDF separator where a silver wire (quasi-

* Corresponding author at: CIRIMAT, Université de Toulouse, CNRS, INPT, UPS, 118 route de Narbonne, 31062 Toulouse Cedex 9, France.
E-mail address: simon@chimie.ups-tlse.fr (P. Simon).

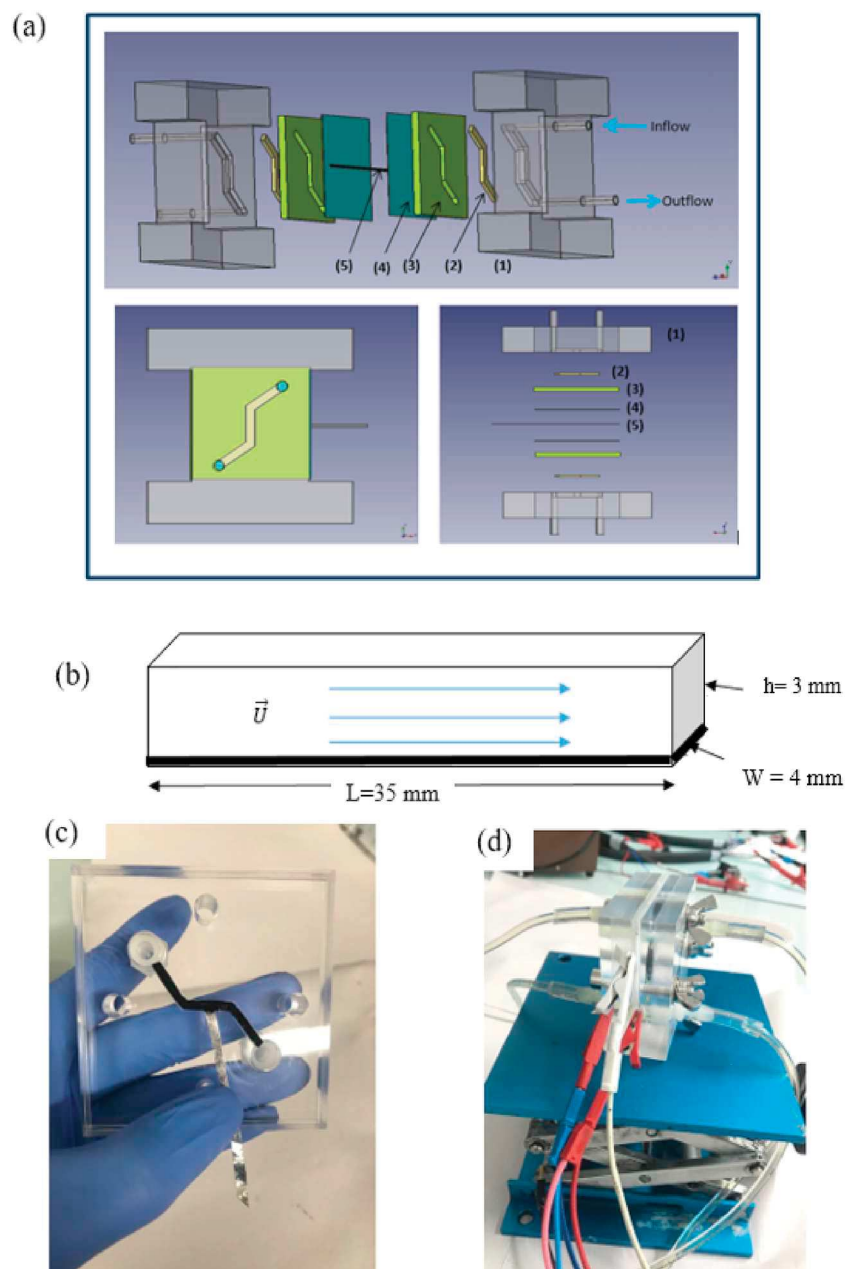


Fig. 1. (a) The different components of the flow cell: (1) plexiglass, (2) Pt current collector, (3) silicone seal, (4) PVDF separator, (5) silver wire (reference electrode). (b) Schematic diagram of a cell compartment considered as a rectilinear channel, with the electrode occupying the whole length and the whole width of the channel. (c) Carbon-coated Pt electrode. (d) whole cell assembly.

reference electrode) is sandwiched in between.

A solution of $2.10^{-3} \text{ mol}\cdot\text{L}^{-1}$ potassium ferricyanide and $0.2 \text{ mol}\cdot\text{L}^{-1}$ potassium sulfate as supporting electrolyte is flown through each compartment at a constant flow rate – from which a flow velocity U (cm/s) can be calculated –, using a peristaltic pump.

Carbon based electrodes were prepared by mixing the activated carbon YP50F or acetylene black (AB, Alfa Aesar, Germany) with poly (vinylidene fluoride-co-hexafluoropropylene) (PVdF-HFP) with a mass ratio of 85:15, in presence of *N*-methyl-2-pyrrolidone (NMP); the slurry obtained was coated by doctor blade on a platinum foil (Fig. 1c). YP50F (Kuraray Chemical Co., Japan) is a microporous activated carbon with a high specific surface area ($1800 \text{ m}^2\cdot\text{g}^{-1}$). The electrodes obtained were dried at 80°C during 4 h under vacuum. YP50F electrode was pressed before use at 2 tons per cm^2 to improve the electrical percolation.

Cyclic voltammograms (CV) measurements were carried out by

using a VMP3 potentiostat (Bio-Logic, France).

3. Results and discussion

In a first step, the cell was assembled using flat Pt electrode foils as both working (WE) and counter electrodes (CE) to study the influence of the scan rate on electrochemical response during constant electrolyte flow experiments (Fig. 2). The cyclic voltammograms (CVs) show nearly no anodic current, as expected from the electrolyte composition, which contains only Fe(+III) species at the initial stage ($\text{Fe}^{\text{III}}(\text{CN})_6^{3-}$), constantly refresh thanks to the flow. Under constant electrolyte flow conditions, the increase of the potential scan rate comes with the increase of the hysteresis of the CVs – current shift between the back and forth potential scan – and leads to the appearance of oxidation and reduction current peaks. The current peaks are observed at 10 mV/s

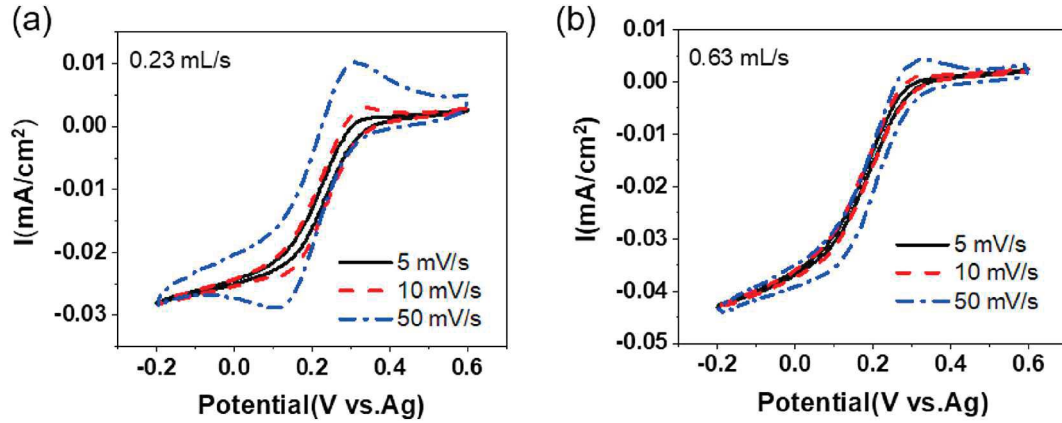


Fig. 2. Effect of the potential scan rate during the polarization of an electrolyte using a Pt foil working electrode at different flow rates of (a) 0.23 mL/s and (b) 0.63 mL/s. The electrolyte contains 200 mM K_2SO_4 as supporting electrolyte and 2 mM $K_3Fe(CN)_6$ as redox probe.

and higher scan rate for a constant flow rate of 0.23 mL/s (Fig. 2a). When the flow rate is increased up to 0.63 mL/s (Fig. 2b), the current peaks are observed at potential scan rates ≥ 50 mV/s. Those results are in line with previous studies which show that, by varying the scan rate and the flow, the change in the mass transport conditions at the electrode surface was responsible for the change of electrochemical signature [16,17].

The presence of peak currents shows that both the redox reaction kinetics and the potential scan rate are fast enough compared to the flow rate. As a result, there is no fast-enough electrolyte renewal inside the electrochemical reaction layer – basically defined as the diffusion layer – during one potential sweep: during cathodic sweep, the produced $Fe^{II}(CN)_6^{4-}$ is still nearby the electrode – in the diffusion layer – leading to the appearance of an anodic peak and an electrochemical signature close to what is expected for a regular CV. Since the flow rate is low – respect to the potential scan rate –, the regime established is not permanent between the convective reactant supplied to the electrode and the electrochemical reaction, leading to a non-stationary domain (non-permanent regime). In this condition, the current depends on the scan rate – the diffusion length is shorter than the hydrodynamic film thickness – and can lead to a poor charge exchange.

A second regime can be defined, where the hysteresis of the curves decreases and current peaks disappear. In this region, the electrolyte flow rate is large enough – respect to the scan rate – to ensure a continuous supply of the reactant to the electrode surface, resulting in the removal of the reaction products. The diffusion occurs within the hydrodynamic film and is now controlled by the flow rate: steady state conditions are established at the electrode surface between the supply of electroactive species by diffusion-convection and the electrochemical reaction, leading to the existence of a permanent domain. This experimental condition should be more desirable to reach an optimum charge conversion and then more efficient desalination.

As a result of the cyclic voltammetry study, two operating regimes can be defined in the cell - non-permanent and permanent - depending on the experimental conditions.

The electrochemical reactions and the flow in the cell are the cause of the existence of two boundary layers [13,18,19]. As previously reported, the presence of a diffusion layer results from the consumption of the electroactive species at the electrode surface. The hydrodynamic layer is the consequence of the flow rate, which leads to the velocity gradient with respect to the distance to the electrode. The frontier which defines the existence of the non-permanent and permanent regimes depends, in a first approach, of the hydraulic diameter which is linked to the cell dimensions and its geometry. To be able to perform a systematic study, it can be helpful to rationalize the experimental parameters. This is why a dimensionless parameter “ θ ” has been defined in order to minimize the influence of the cell design, to anticipate

what will be the cell regime in order to get the most efficient charge exchange and potentially the best desalination operating conditions. The dimensionless number “ θ ” has been defined as the ratio between the scan time t_{st} (s) of the potential and the turnover time of the electrolyte t_{to} (s).

$$\theta = \frac{t_{st}}{t_{to}} \quad (1)$$

The scan time of the potential t_{st} is given by the Eq. (2), which is a ratio between the potential difference ΔE (V) and the scan rate (V/s)

$$t_{st} = \frac{\Delta E}{sr} \quad (2)$$

The turnover time t_{to} can be defined using equation as follow:

$$t_{to} = \frac{L}{U} \quad (3)$$

where L (m) is the length of the channel, U (m/s) is the flow velocity.

The velocity is given by:

$$U = \frac{4}{\pi d_h^2} \times Q \quad (4)$$

where Q is the flow rate ($m^3 \cdot s^{-1}$), and d_h , the hydraulic diameter (m). The latter can be expressed as:

$$d_h = \frac{4 \times S}{P} = \frac{2(h \times W)}{(h + W)} \quad (5)$$

where S and P are respectively the cross-sectional area (m^2) of the flow and the wetted perimeter (m) [20].

From Eqs. (1), (2), (3) and (4) θ as:

$$\theta = \frac{4\Delta E}{\pi L d_h^2} \times \frac{Q}{sr} \quad (6)$$

The dimensionless number θ changes with the flow rate and is inversely proportional to the potential scan rate.

The dimensionless number θ is used to define the different flowing regimes in the cell: the boundaries conditions between the permanent and the non-permanent domain can be set according to the value of θ . From Fig. 2, it is possible to define the existence of a non-permanent regime for $\theta < 45 \pm 15$. Indeed, for the CVs whose peak current is observed, the calculation gives $\theta = 57$ and $\theta = 11$ respectively for the scan rates of 10 and 50 mV/s at 0.23 mL/s (Fig. 2a), and for 0.63 mL/s (Fig. 2b) the peak current is obtained at 50 mV/s corresponding to $\theta = 31$, which as mentioned before correspond to the non-permanent domain. Then, for $\theta > 45 \pm 15$ corresponds to the permanent domain: $\theta = 114$ (5 mV/s) at 0.23 mL/s (Fig. 2a) and for 0.63 mL/s (Fig. 2b) $\theta = 313$ (5 mV/s), $\theta = 156$ (10 mV/s).

In summary, from these results, we can define the boundary

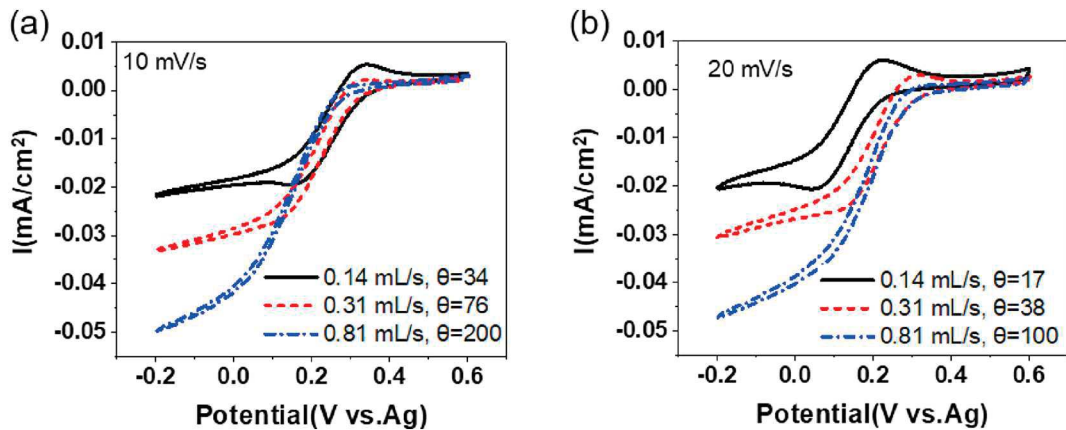


Fig. 3. Effect of the flow rate during the polarization of an electrolyte using a Pt foil working electrode at constant potential scan rate of (a) 10 mV/s and (b) 20 mV/s. The electrolyte contains 200 mM K_2SO_4 as supporting electrolyte and 2 mM $K_3Fe(CN)_6$.

between the permanent domain and the non-permanent domains at about $\theta = 45 \pm 15$ at a constant flow. Beyond this value, the current is directly proportional to the flow rate and there is no hysteresis anymore. To confirm this behavior, experiments have been achieved at a constant potential rate for different electrolyte flow rates and the results are presented in Fig. 3.

In Fig. 3 is shown that the increase in the flow rate at constant potential scan rate (an increase of θ , see Eq. (6)) leads to a decrease in the hysteresis of the CV together with a disappearance of the current peaks and an increase in the diffusion limiting current – plateau current. Considering a constant scan rate of 10 mV/s (Fig. 3a), the current peak appears at a flow rate of 0.14 mL/s (that is, $\theta = 34$) but disappears with larger flow rate (0.31 mL/s and 0.81 mL/s corresponding respectively to $\theta = 76$ and $\theta = 200$). Interestingly, when the sweep rate is increased to 20 mV/s in Fig. 3b, the current peaks can be also observed for a flow rate of 0.31 mL/s ($\theta = 38$). These results are consistent with constant flow experiments results where two different regimes were observed depending on θ value. Here again, for $\theta < 45 \pm 15$, the existence of a non-permanent regime is responsible for the appearance of redox peaks due to the diffusion-controlled reaction kinetics. When $\theta > 45 \pm 15$, these current peaks disappear in agreement with the establishment of a steady-state regime between the reactant supply to the electrode by convection and the consumption by the electrochemical reaction, where the current depends on the flow rate.

In summary, the measurements achieved with a Pt foil working electrode have shown the existence of two operating domains in our cell. The existence of these domains can be predicted by the use of the dimensionless quantity θ (Eq. (6)), which is independent of the cell design. However, capacitive desalination cell operates under standard conditions with high surface area porous carbon as electrodes, and not using a Pt foil electrode. As a result, we have investigated the behavior of the cell operating first with carbon black (AB), which has a larger external surface area ($64 \text{ m}^2/\text{g}$) than platinum, and second with YP50F, which is a porous carbon with high specific surface area ($1732 \text{ m}^2/\text{g}$). The dimensionless quantity θ was used to characterize the flow regime in the cell.

Fig. 4 shows the comparison of the electrochemical signature of Pt and AB electrodes in static mode, as a starting point. The CVs shapes are the same for both electrodes, but the current is greater with AB, in agreement with the higher specific surface of the carbon black film compared to Pt. Thus, the current peak observed with the AB electrode ($0.26 \text{ mA}/\text{cm}^2$) is significantly higher than the current peak of the Pt electrode ($0.03 \text{ mA}/\text{cm}^2$).

Fig. 5 shows the electrochemical characterization of the carbon black film coated on a platinum electrode in flow mode. As previously made, we used the dimensionless quantity θ to identify the mass transfer regime in the cell. Fig. 5a and b show the effect of the scan rate

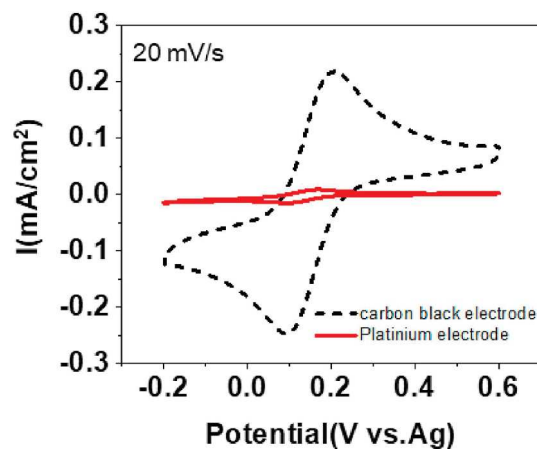


Fig. 4. Cyclic voltammetry of a platinum electrode and a platinum electrode coated with a carbon black film (85% AB-15%PVDF-HFP). The electrolyte contains 200 mM K_2SO_4 as supporting electrolyte and 2 mM $K_3Fe(CN)_6$.

on the electrochemical signature at a constant flow rate of 0.45 mL/s (Fig. 5a) and 0.81 mL/s (Fig. 5b). At 0.45 mL/s, the current peaks appear for scan rate higher than 20 mV/s, corresponding to θ value ≤ 56 . Similarly, at 0.81 mL/s, the current peaks appear at 50 mV/s and higher, corresponding to a value of $\theta \leq 40$. These results confirm that, as previously observed with the Pt foil working electrode, the dimensionless quantity θ is the border between two different regimes: a non-permanent regime for $\theta < 45 \pm 15$ and a permanent regime for $\theta > 45 \pm 15$ for porous carbon electrodes.

Fig. 5c and d show the effect of the change of the flow rate on the electrochemical signal at constant scan rates of 10 mV/s and 20 mV/s, respectively. At 10 mV/s, the current peaks are observed only for $\theta = 34$, corresponding to a flow rate of 0.14 mL/s. When the scan rate is increased to 20 mV/s, the current peaks appear at flow rates of 0.14 mL/s and 0.31 mL/s corresponding to $\theta = 17$ and $\theta = 38$, respectively. As in the case of the experiments carried out with the platinum electrode at a constant speed, we also observe the existence of 2 domains in the function of the value of θ , and the change of regime was observed at the same value of $\theta = 40 \pm 15$.

In a last series of experiments, high-surface area activated carbon YP50F coated onto Pt foil and CVs are presented in Fig. 6. As previously observed current peaks appear for regime defined by $\theta 45 \pm 15$, that is at high flow rates, even though the high capacitive current tends to take over. One can notice anyway that the higher the θ , the higher the reduction current is between 0.2 V and -0.2 V, which, as previously, is ascribed to the ferricyanide reduction. It can also be observed that the

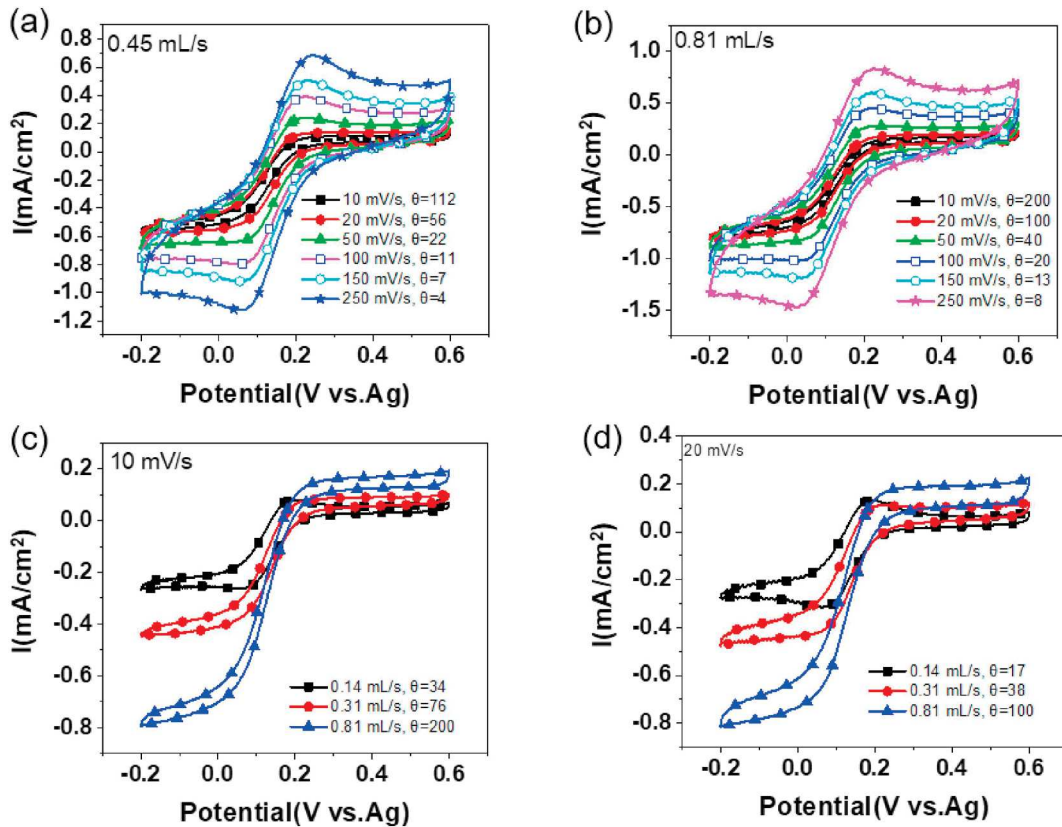


Fig. 5. Cyclic voltammetry of a carbon black electrode film (85% AB-15%PVDF-HFP) in a 2 mM + 200 mM electrolyte. Effect of the scan rate with a constant flow rate of 0.45 mL/s (a) and 0.81 mL/s (b). (c) Influence of the flow rate at a constant potential scan rate of 10 mV/s. (d) Influence of the flow rate at a constant potential scan rate of 10 mV/s. The electrolyte contains 200 mM K_2SO_4 as supporting electrolyte and 2 mM $K_3Fe(CN)_6$.

capacitive current – between 0.2 V and 0.6 V is not influenced by the flow rate, which is consistent since it is driven by the electrochemical double layer formation. As observed before, current peaks are observed at 0.14 mL/s, corresponding to $\theta = 34$. With increasing the flow θ increases and the current peak disappears. A more efficient desalination will be achieved for experimental parameters allowing for a high ionic charge exchange.

Fig. 7 shows the logarithmic change of the charge q with θ for the various electrode configurations: bare Pt, AB covered Pt and AC covered Pt. A charge increases according to θ is observed. Beyond $\theta = 45$, the charge tends to a constant value corresponding to the permanent domain. As mentioned earlier, this study aims to have optimal charge conversion and better desalination. Fig. 7 clearly shows that the most efficient regime for NaCl salt removal from salted water is the

permanent domain corresponding to the highest charge conversion. Also, as expected, a higher charge exchange is measured while the specific surface area of the electrode is increased. Nevertheless, the activated carbon-based electrode exhibits a lower dependency with θ , as compared to Pt and AB electrodes. Those results are consistent with that, in such materials, the charge exchanged through the electrochemical double layer within the porosity – capacitive current – reaches a similar value as the reduction current of the ferricyanide.

In summary, this study shows that the definition of the dimensionless number θ allows the prediction of the mass transfer regime in a flow cell, whatever the cell dimension. Thanks to this quantity, flow parameters can be anticipated to get efficient charge adsorption which was identified here as the permanent domain ($\theta > 40 \pm 15$).

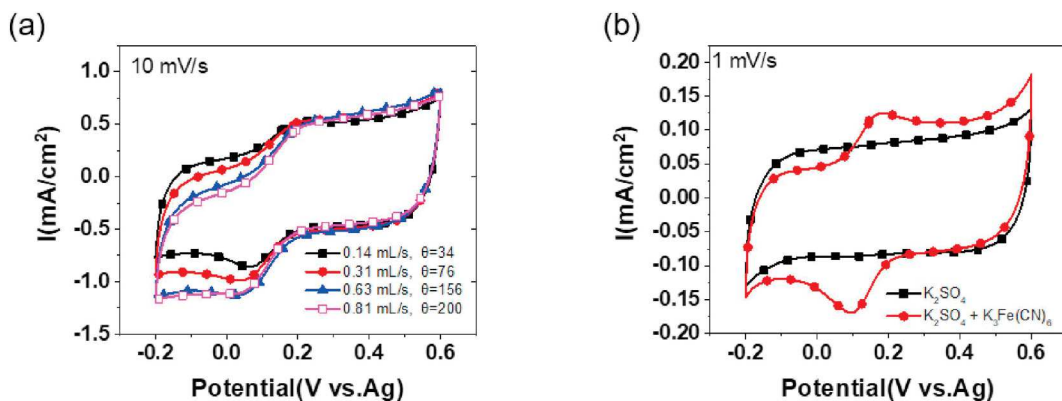


Fig. 6. Cyclic voltammograms of a YP50-F film coated onto a platinum electrode (85% YP50F-15%PVDF-HFP). (a) Influence of the flow rate at a constant potential scan rate of 10 mV/s. (b). The electrolyte contains 200 mM K_2SO_4 as supporting electrolyte and 2 mM $K_3Fe(CN)_6$.

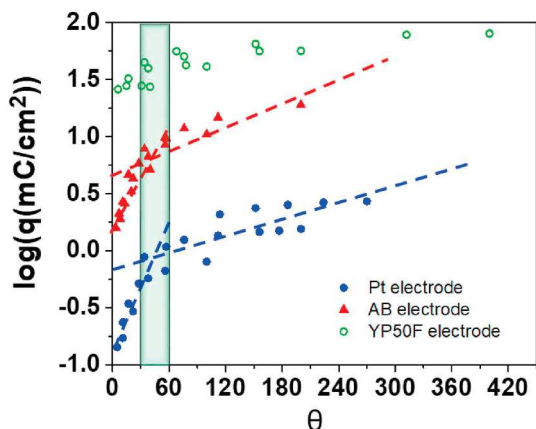


Fig. 7. Logarithmic evolution of the charge q with θ .

4. Conclusion

The purpose of our study was to characterize a desalination cell using different type of electrode. Two operating regimes have been evidenced, depending on the potential scan rate and the electrolyte flow rate. When the electrochemical reaction is fast enough with respect to the convection of the electroactive species on the surface of the electrode, a non-permanent regime is achieved, where the reactions are purely controlled by the diffusion of the species to the electrode surface. Differently, a permanent domain is established when the electrolyte flow rate is high enough vs the potential scan rate to ensure a continuous supply of the reactant to the electrode surface. In this work, a dimensionless quantity θ has been defined which is expressed as a function of the flow rate and the scan rate, which is independent of the cell dimensions. We have used the value of θ to determinate the boundary between two operating modes of the cell. It has been shown that a permanent regime was observed for $\theta > 40 \pm 15$ and a non-permanent domain for $\theta < 40 \pm 15$. Similar behavior was observed when replacing the Pt foil working electrode by an AB-coated Pt electrode although the current was much larger with the AB electrode due to the high surface area. Increasing the electrode surface by using activated carbon-coated Pt electrode came with an important increase of the capacitive current in addition to the faradaic current. The use of the dimensionless θ quantity will help in better understand the best mass transfer conditions needed to achieve efficient desalination using our cell in a flow mode where a carbon slurry will circulate in the cell.

Acknowledgment

P.S. and P.-L.T. thank the ANR (Agence Nationale de la Recherche),

Labex STORE-EX program for funding.

References

- [1] S.L. Postel, G.C. Daily, P.R. Ehrlich, Human appropriation of renewable fresh water, *Science*, New Series 271 (5250) (1996) 785–788.
- [2] D. González, J. Amigo, F. Suárez, Membrane distillation: perspectives for sustainable and improved desalination, *Renew. Sust. Energ. Rev.* 80 (2017) 238–259.
- [3] M. Chérif, I. Mkacher, L. Dammak, A. Ben Salah, K. Walha, D. Grande, V. Nikonenko, Water desalination by neutralization dialysis with ion-exchange membranes: flow rate and acid/alkali concentration effects, *Desalination* 361 (2015) 13–24.
- [4] S. Zhao, L. Zou, D. Mulcahy, Brackish water desalination by a hybrid forward osmosis–nanofiltration system using divalent draw solute, *Desalination* 284 (2012) 175–181.
- [5] M.A. Anderson, A.L. Cudero, J. Palma, Capacitive deionization as an electrochemical means of saving energy and delivering clean water. Comparison to present desalination practices: will it compete? *Electrochim. Acta* 55 (12) (2010) 3845–3856.
- [6] Y. Oren, Capacitive deionization (CDI) for desalination and water treatment — past, present and future (a review), *Desalination* 228 (1) (2008) 10–29.
- [7] T.J. Welgemoed, C.F. Schutte, Capacitive deionization technology™: an alternative desalination solution, *Desalination* 183 (1) (2005) 327–340.
- [8] M.E. Suss, S. Porada, X. Sun, P.M. Biesheuvel, J. Yoon, V. Presser, Water desalination via capacitive deionization: what is it and what can we expect from it? *Energy Environ. Sci.* 8 (8) (2015) 2296–2319.
- [9] S. Porada, R. Zhao, A. van der Wal, V. Presser, P.M. Biesheuvel, Review on the science and technology of water desalination by capacitive deionization, *Prog. Mater. Sci.* 58 (8) (2013) 1388–1442.
- [10] F.A. AlMarzooqi, A.A. Al Ghaferi, I. Saadat, N. Hilal, Application of capacitive deionization in water desalination: a review, *Desalination* 342 (2014) 3–15.
- [11] M. Mossad, L. Zou, A study of the capacitive deionisation performance under various operational conditions, *J. Hazard. Mater.* 213 (2012) 491–497.
- [12] B. Jia, W. Zhang, Preparation and application of electrodes in capacitive deionization (CDI): a state-of-art review, *Nanoscale Res. Lett.* 11 (1) (2016).
- [13] J. Newman, K.E. Thomas-Alyea, *Electrochemical Systems*, John Wiley & Sons, 2012.
- [14] P.M. Biesheuvel, Y. Fu, M.Z. Bazant, Diffuse charge and Faradaic reactions in porous electrodes, *Phys. Rev. E* 83 (6) (2011) 061507.
- [15] J.S. Newman, C.W. Tobias, Theoretical analysis of current distribution in porous electrodes, *J. Electrochem. Soc.* 109 (12) (1962) 1183–1191.
- [16] C. Amatore, C. Pebay, L. Thouin, A. Wang, Cyclic voltammetry at microelectrodes. Influence of natural convection on diffusion layers as characterized by in situ mapping of concentration profiles, *Electrochem. Commun.* 11 (6) (2009) 1269–1272.
- [17] B.J. Adesokan, X. Quan, A. Evgrafov, A. Heiskanen, A. Boisen, M.P. Sørensen, Experimentation and numerical modeling of cyclic voltammetry for electrochemical micro-sized sensors under the influence of electrolyte flow, *J. Electroanal. Chem.* 763 (2016) 141–148.
- [18] L. Petit, J.-P. Hulin, É. Guyon, *Hydrodynamique physique 3e édition*, EDP Sciences, 2012, p. 2012.
- [19] C. Amatore, S. Szunerits, L. Thouin, J.-S. Warkocz, The real meaning of Nernst's steady diffusion layer concept under non-forced hydrodynamic conditions. A simple model based on Levich's seminal view of convection, *J. Electroanal. Chem.* 500 (1) (2001) 62–70.
- [20] X.F. Peng, G.P. Peterson, Convective heat transfer and flow friction for water flow in microchannel structures, *Int. J. Heat Mass Transf.* 39 (12) (1996) 2599–2608.